



Thermomechanical behaviour of Al₂O₃–MgO–C refractories under non-oxidizing atmosphere

Vanesa Muñoz, Analía Gladys Tomba Martínez*

Instituto de Investigaciones en Ciencia y Tecnología de Materiales (INTEMA), CONICET – Facultad de Ingeniería/Universidad Nacional de Mar del Plata, Avenida J.B. Justo 4302, 7600 Mar del Plata, Argentina

Received 23 September 2014; received in revised form 22 October 2014; accepted 24 October 2014
Available online 11 November 2014

Abstract

Al₂O₃–MgO–C (AMC) refractory bricks are used as linings for the sidewalls (metal line) and bottoms of steel-making ladles. As a structural component of this type of vessel, these bricks undergo mechanical and thermal loading in service. For this reason, knowledge about their thermo-mechanical behavior is needed for material selection and ladle design using structural calculus. Even when the mechanical response of AMC refractories is similar to that of MgO–C bricks, which have been studied a great deal, they have distinctive features that have to be studied specifically. The aim of this paper is to evaluate the mechanical performance of three commercial Al₂O₃–MgO–C bricks by stress–strain curves from RT to 1260 °C, using a non-oxidizing atmosphere (nitrogen). From these curves, the following mechanical parameters were determined: apparent Young' modulus (E), mechanical strength (σ_R), fracture strain (ϵ_R) and yield stress (σ_Y). In order to infer what the main factors are in determining the mechanical response of each AMC refractory, the tested specimens were analyzed by bulk density and apparent porosity measurements and SEM/EDS. The increasing porosity (pores and microcracks), the loss of graphite and the new solids formed as products of the reactions between the refractory components control the behavior of the studied AMC materials. However, the contribution of each depends on the temperature and the refractories' characteristics.

© 2014 Elsevier Ltd and Techna Group S.r.l. All rights reserved.

Keywords: C. Mechanical properties; D. Al₂O₃; D. Carbon; D. MgO; E. Refractories

1. Introduction

Al₂O₃–MgO–C (AMC) refractory bricks, which emerged in the 1980s as an alternative to MgO–C and Al₂O₃–C bricks, are used as linings for the sidewalls (metal line) and bottoms of steel-making ladles. As a structural component of these vessels, these bricks undergo mechanical and thermal loading in service. For this reason, knowledge about their thermo-mechanical behavior is needed for material selection and ladle design using structural calculus. Even when the mechanical response of AMC refractories is similar to that of other members of oxide–C bricks' group (such as MgO–C bricks, which have been studied a great deal) they have distinctive features that have to be studied specifically.

The complexity inherent to the mineralogy, microstructure and texture of oxide–C refractory bricks leads to a complex behavior of such materials under mechanical loading. Some of the mechanical characteristics of oxide–C refractories are [1] the non-linear stress–strain relationship in tension as well as in compression, stiffness loss during loading, a residual strain in the unloading, and a strong dependency with temperature affected by chemical-reactions products, showing a quasi-brittle behavior in the low temperature range and appearance of viscoplasticity at high temperature. These particularities determine the performance of carbon-containing bricks and in some cases, can even limit their lifetime.

The graphite flakes have a fundamental role in the typical mechanical behavior of oxide–C refractories. Due to the cleavage on the basal plane and the lack of any directional bonding on the plane, which makes sliding between flakes

*Corresponding author. Tel.: +54 223 4816600; fax: +54 223 4810046.
E-mail address: agtomba@fi.mdp.edu.ar (A.G. Tomba Martínez).

easier, and the crumpling of flakes, graphite particles themselves are extremely flexible and have non-linear deformation [2]. As a consequence, these particles are partially responsible for the non-linearity of the stress–strain relationship, the flexibility and the high strain to fracture exhibited by carbon-containing refractories. Flexibility, defined as the ability to absorb stress [3], is a desired property from a thermomechanical point of view along with resistance to crack propagation (toughness); it is thus favored in processes that absorb energy. The capacity to relieve stresses in graphite products leads to the viscoplasticity displayed by these materials, even at small loads and room temperature [4]. On the other hand, some authors consider graphite flakes as critical flaws [5]; during the mechanical loading, and after the particles have been deformed (along their basal planes) and slip (lubricant effect), cracks are formed along and perpendicular to the flakes. Another source of microcracks and associated non-linear stress–strain relationship of graphite-containing bodies are the Mrozowski cracks present into the flakes (formed by differential thermal contraction during the graphitization process [2]), which play a role in mechanical response because they can close when the brick is heated.

Besides those associated with graphite flakes, the matrix of oxide–C brick has additional microcracks [2]. During loading, fissures (independent of their origin) extend causing damage accumulation, which contribute to the non-linearity of stress–strain curves. Microcracks can also be created during the mechanical loading. The cracks extend mainly within the matrix and rounding aggregates [5], given that the interfaces between the bonding phase and the coarse particles are weak points in the structure [6]. Other contributions to the non-linear behavior of this type of material are the microplasticity of the organic binder and the relief of residual stresses introduced during brick manufacture [2,5,7]. At higher temperatures, other mechanisms for non-linearity are due to differences between the thermal expansion coefficients of the aggregates and the matrix, which could lead to microcracking, and the appearance of a certain amount of ductility due to all the refractory's components becoming more viscoplastic [5].

Another remarkable aspect of the mechanical behavior of these refractories is the thermal dependency, which has been widely studied by several authors for MgO–C bricks, with and without antioxidants [5–17]. The influence of the microstructural and textural evolution caused by the reactions taking place within the material (carbonization of the organic binder, direct graphite oxidation, formation of carbide, nitride or oxides, spinel formation) has been well established.

According to the major work done studying the deformation and fracture mechanisms [8–11,14,15], the mechanical behavior of MgO–C bricks in the medium range of temperatures (RT–1000 °C) is determined by changes in the porosity/microcracks due to the transformation of the organic binder (pitch or resin) and the loss of graphite. Both processes diminish the mechanical performance, bearing in mind the above-mentioned benefits provided mainly by graphite. Above 1000 °C, behavior depends on if antioxidants are present or not in the composition of the brick; one of the most studied additives is aluminum. This agent reacts with other components to form new phases such as Al_4C_3 , AlN, Al_2O_3

and $MgO \cdot Al_2O_3$ spinel, depending on the temperature and atmosphere. These new solids could contribute to enhancing the mechanical response (besides inhibiting direct graphite oxidation) up to 1400–1500 °C. The increase in the mechanical strength due to the Al_4C_3 formed in MgO–C materials with aluminum (2.5 and 5.0 wt%) in the range between 1000 and 1500 °C (argon atmosphere) has been attributed to the plate or skeletal shape of the carbide particles [13,14,18]. As for spinel, Baudín et al. [14] found an increase in the modulus of rupture (HMOR) between 1200 and 1450 °C, which was related to crack sealing by the crystallized spinel particles. Taffin and Poirier [18] also detected an increase in this parameter between 1300 and 1500 °C, but they attributed this fact to the more compact structure of spinel compared to that of the carbide it replaces.

Several of the aspects analyzed and reported for MgO–C also apply to Al_2O_3 –MgO–C (AMC) refractories, for which there are not as many reports or such a deep level of analysis [19]. The mechanical degradation of AMC refractories, strongly depends on the range of temperature and the gases composing the atmosphere, very similar to what happens with MgO–C bricks. Moreover, this degradation is influenced by the composition, microstructure and texture of the refractories, but the presence of Al_2O_3 imposes some differences, such as the relevance of spinel formation. For this reason, and since reports pertaining to AMC refractories are scarce, it is necessary to establish the particular characteristics of these materials in relation to their mechanical behavior for both technological and scientific demands.

Taking into account the convenience of having a complete stress–strain curve (s–s) for the mechanical evaluation of oxide–C refractories (in comparison with more frequently used tests to determine one parameter such as MOR, MOE, HMOR, HMOE), this methodology is used here to study the behavior of commercial AMC of different qualities. Compressive loading is applied in the mechanical tests, because it avoids the problems associated to tension in brittle materials. Moreover, compressive stresses are prevalent in refractory structures, especially in oxide–C bricks structures [20]. However, the compression testing has disadvantages already known, such as the friction in the contact area between the specimen and the platens, whose effects on the s–s curve testing has been discussed in a previous work of the authors [21]. The present study looks at the particularities of each AMC material under mechanical loading, from RT to 1260 °C, in a non-oxidant atmosphere, and the main determining factors. Beyond the specific behavior of the evaluated AMC bricks, the study attempts to find relationships among microstructure–texture–properties that could be extended to other refractories of the same group.

2. Experimental procedure

2.1. Materials

Three Al_2O_3 –MgO–C commercial refractory bricks manufactured by the same supplier and labeled as AMC1, AMC2 and AMC3 were analyzed. The bricks each have a different MgO content and type of raw material used as the source of alumina.

Bearing in mind the aim of this work, these materials were exhaustively characterized using a vast group of analytical techniques: X-ray fluorescence (XRF), plasma emission spectroscopy (ICP-OES), gravimetry, X-ray diffraction (XRD), differential thermal and thermogravimetric analyses (DTA/TGA), reflection optical microscopy and scanning electron microscopy coupled with X-ray dispersive energy (SEM/EDS), measurements of density and porosity, Hg-intrusion porosimetry, dilatometric analysis and permanent linear change (PLC). The results of the refractories' characterization have been previously reported [22], and the main data are summarized in Table 1.

From these analyses, it was determined that every refractory contains brown electrofused alumina (EF) plus tabular alumina (TA). AMC1 has a higher proportion of TA aggregates to EF aggregates, as well as a higher proportion of TA aggregates compared to the other two materials. Furthermore, it was confirmed that only AMC3 possesses bauxite, and that aluminum is used as an antioxidant in all three materials in similar proportions. The higher amount of sintered magnesia in AMC2 is distributed in the medium-fine fraction whereas this component is present only as fine particles in the matrix in AMC1 and AMC3.

Graphite, whose particles have a similar aspect ratio in the three materials, has a higher content in AMC2, but its flakes are the smallest. The amount of graphite in AMC3 is somewhat lower and its particles are the purest, which leads to the higher temperature of the DTA peak corresponding to the graphite oxidation, in comparison with the temperature of the peaks displayed in the other two refractories. The bricks contain a similar amount of resin as organic binders, although it was not possible to determine what kind of phenolic resins they are (novolaka or resol).

Regarding the texture, AMC2 has a larger amount of open pores, although they are similar in size to those of AMC1. AMC3, however, has the lowest values of open porosity, permeability and pore size.

The dilatometric analysis of the refractories showed that the expansion of AMC3 was less than the other two materials. This fact indicates that, for AMC3: (a) the global thermal expansion coefficient (α) was smaller, (b) the expansive reactions (mainly the formation of spinel) had occurred to a lower degree and/or

(c) the microstructure of the material had accommodated volumetric changes in a more efficient way by mechanisms such as the crystallization of new phases into pores, microcracking or sliding of the material by viscous flow of low melting point phases. The presence of $AlTi_2O_4$ in the bauxite aggregates surely reduces the value of the global α of AMC3. On the other hand, the higher amount of impurities in this refractory could encourage the presence of low melting point phases that assist the sliding of particles at high temperatures.

2.2. Methodology

The response to thermal and mechanical loadings of AMC bricks was studied by the measurement of stress–strain curves in compression, at room temperature (RT), 700, 1000 and 1260 °C, in a non-oxidant atmosphere (nitrogen), using an experimental protocol specially designed for oxide–C refractories [21,23].

An Instron 8501 servohydraulic testing machine coupled with an SFL electric furnace ($MoSi_2$ heating elements) was used for mechanical testing. The tests were carried out by displacement control, with a constant rate of 0.1 mm/min up to the specimen's failure. Cylinders were used measuring 27 mm in diameter and 40 mm in height, which were obtained by cutting the bricks and machining flat faces. A continuous flow (5 l/min) of N_2 gas (99.995%) was selected, which represents a compromise between efficiency to reduce graphite loss by direct oxidation with oxygen from the atmosphere, and cost [21]. The axial displacement of the cylinders was measured with an Instron capacitive extensometer ($\pm 0.6 \mu m$) for high temperature testing. Mechanical tests were carried out by duplicate at least, although in most of cases more than two nominally identical specimens were evaluated (up to four) in order to obtain repetitive s–s curves.

Fracture features as well as changes occurring in the specimens were also analyzed. Bulk density and apparent porosity were measured for fragments of the tested cylinders, with a methodology based on the DIN 51056 standard [24] using kerosene as the known density fluid and a Sartorius BP 221S analytical balance (± 0.0001 g). SEM/EDS analysis was also performed on cross surfaces of tested specimens previously packed in vacuum with a polyester resin and which were transversally cut, ground and polished (up to 3 μm diamond paste). The systematic analysis of

Table 1
Composition and physical properties of AMC refractories.

		AMC1	AMC2	AMC3
Main phases (wt%)	Corundum (Al_2O_3)	82.7 \pm 0.3	57.6 \pm 0.3	70.5 \pm 0.3
	Periclase (MgO)	5.40 \pm 0.02	27.0 \pm 0.1	6.8 \pm 0.1
Secondary phases (wt%)	Graphite (C)	1.7 \pm 0.1	3.5 \pm 0.1	3.0 \pm 0.1
	Resin (C, O, H)	5.4 \pm 0.1	5.6 \pm 0.1	5.0 \pm 0.1
	Aluminum (Al)	1.39 \pm 0.02	1.37 \pm 0.02	1.60 \pm 0.02
		3.14 \pm 0.02	2.98 \pm 0.01	3.14 \pm 0.1
Bulk density (kg/m^3)		6.7 \pm 0.1	7.8 \pm 0.5	4.0 \pm 0.1
Apparent porosity (%)		10 \pm 2	12 \pm 2	7 \pm 2
Total porosity (%)		0.013	0.015	0.008
Permeability ($m^3/Nw/s$) ^a		1.1	0.8	0.3
$\Delta l/l_0^{1260^\circ C}$ (%) ^b				

^aFor ΔP of 3 MPa.

^bFrom dilatometric analysis in argon.

the microstructures were carried out only at 1000 and 1260 °C due to the formation of new phases occurring above 1000 °C according to the DRX mineralogical and thermal evolution analyses of these materials [25].

The following parameters were obtained from the σ – ϵ curves: the apparent Young's modulus (E), calculated as the slope of the linear part of the curve, the mechanical strength (σ_R), corresponding to the value of stress for the maximum load, the fracture strain (ϵ_R), which is the strain corresponding to the maximum load, and the yield stress (σ_Y), defined as the stress where the curve deviated from linear behavior. The ratio σ_Y/σ_R , expressed as a percentage, was calculated as an indication of the degree of non-linearity of the refractory's mechanical behavior.

3. Results

3.1. Stress–strain mechanical tests

Typical σ – ϵ curves of each of the AMC refractories at different testing temperatures are shown in Fig. 1. As example, σ – ϵ curves for nominal identical specimens of AMC3 tested at 1260 °C are plotted all together in Fig. 2. Taking into account the high inherent dispersion expected for mechanical properties in such heterogeneous materials, these three curves were considered representative of the material's stress–strain relationship at the testing temperature. Mechanical parameters vs. testing temperature are plotted in Figs. 3 and 4, where error bars correspond to standard deviations. Lines are used to connect the media values for clarity only and do not indicate the change in the respective parameter with temperature.

Stress–strain curves show the quasi-brittle behavior characteristic of oxide–C refractories, and softening (the stress drops gradually after the maximum, with a loss of stiffness) is also observed in some cases. The degree of deviation from the linear response and the degree of softening depend on the particular AMC refractory and the testing temperature. With respect to the mechanical parameters, some tendencies, such as the notable reduction of the mechanical strength at 700 °C and its recovery at higher temperatures, were similar for the three materials. The evolution of the apparent Young's modulus, the fracture strain and the σ_Y/σ_R ration depended, to more or less degree, on the refractory's characteristics.

Fracture occurred at 45° (indicating unavoidable frictional effects during the test) in most of the tested specimens, propagating through the matrix and around the aggregates in several cases. This fact demonstrates the fundamental role of the bonding phase in the mechanical behavior of this type of refractory because it is the weakest link of the structure itself as well as the interface with the aggregates. Except AMC3 specimens when they were mechanically tested at 700 °C, the superficial decarburization of the cylinders was evident in the rest of the cases.

3.2. Post-testing characterization

3.2.1. Bulk densities and apparent porosity measurements

Plots of the variation of the bulk density and apparent porosity of the tested specimens as the testing temperature

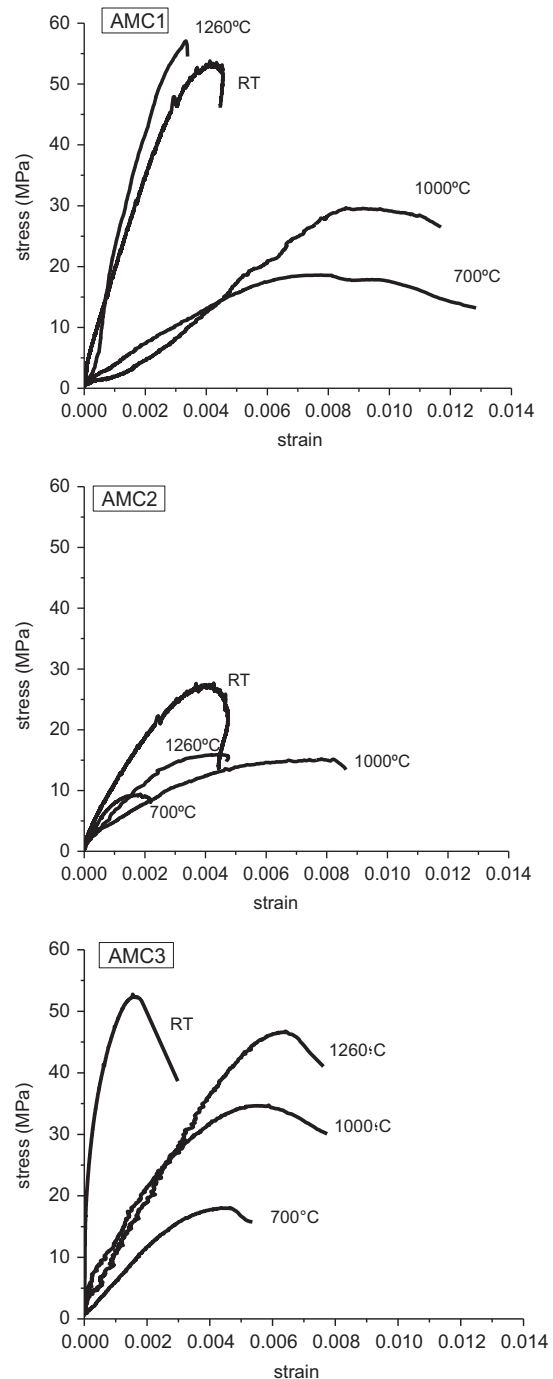


Fig. 1. Typical σ – ϵ curves of AMC refractories at different testing temperatures.

increased are shown in Fig. 5, where bars correspond to standard deviations. Lines are used to connect the media values for clarity only and do not indicate the change in the respective parameter with temperature.

The volumetric fraction of open pores increases gradually as the testing temperature rises. According to previous characterization of the three AMC refractory bricks [22,25], resin transformation occurs between 350 and 700 °C, and graphite oxidation begins from the last temperature, with both processes being the main sources of porosity (pores and microcracks) in these refractories. At higher temperatures (> 1000 °C), the contributions of the oxidation of

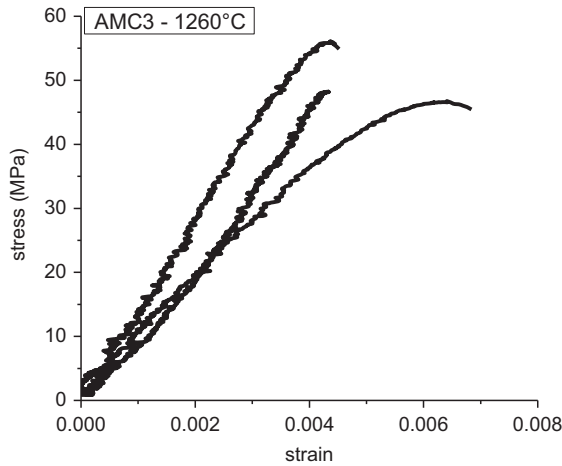


Fig. 2. Stress–strain curves for nominal identical specimens (AMC3, 1260 °C).

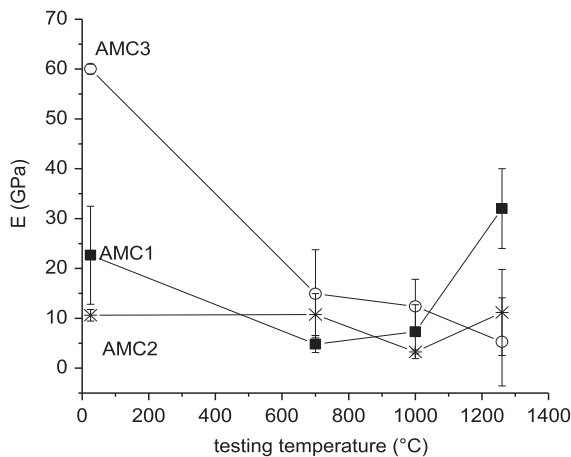
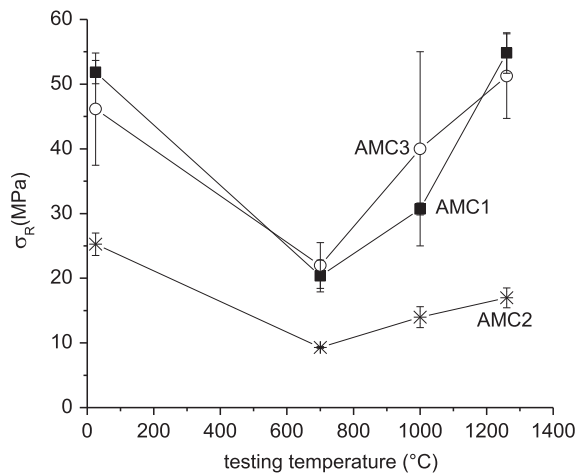


Fig. 3. Variation of the mechanical strength (σ_R) and the apparent Young's modulus (E) of AMC refractories with the testing temperature.

impurities and, according to the reaction mechanism, the spinel formation, could also add [14,15]. Spinel formation by more than one mechanism, such as the following:

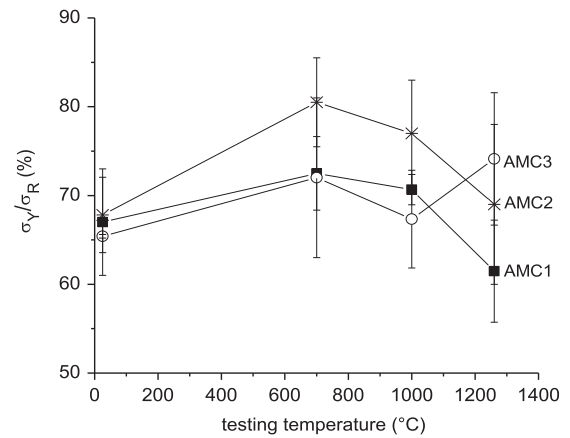
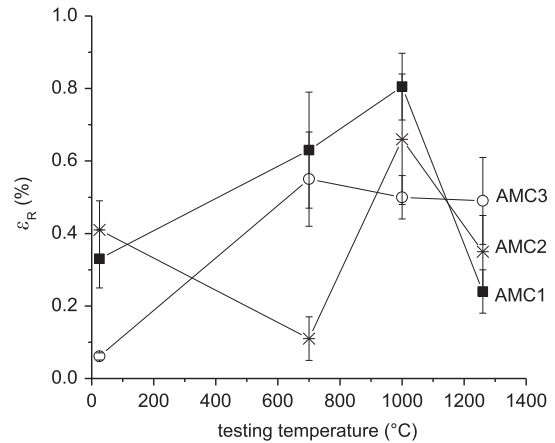
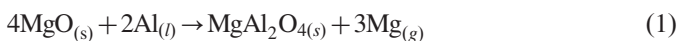
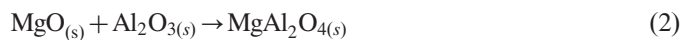


Fig. 4. Variation of fracture strain (ε_R) and σ_Y/σ_R percentage ratio of AMC refractories with testing temperature.



was confirmed in AMC1, AMC2 and AMC3 from 1000 °C [22,25].

The difference in the apparent porosity between AMC1 specimens tested at 700 and 1000 °C is not significant taking into account the experimental error; similar unchanged values are observed in the case of AMC2 specimens tested at these temperatures. This fact could be related to a possible reduction in open porosity in the outer layers of the cylinders due to the formation of sub-products such as soot (from: $2\text{CO} \rightarrow \text{CO}_2 + \text{C}_{(s)}$) [26] and the closure of open micropores by resin transformation [27]. The higher susceptibility to oxidation manifested by AMC1 and AMC2 refractories, and the way this process advances in this range of temperature (which has been previously reported by the authors [28]), brings support to this hypothesis. On the other hand, AMC3 retained values of open porosity smaller than those of the other two refractories up to 1000 °C, when it matched them. The remarkable increase in the apparent porosity of AMC3 between 700 and 1000 °C is due to the oxidation of graphite, which just begins in this range of temperatures due to the inherent resistance of its flakes and the lower volumetric fraction of open pores and permeability of the original brick, as was reported in a previous work of the authors [22].

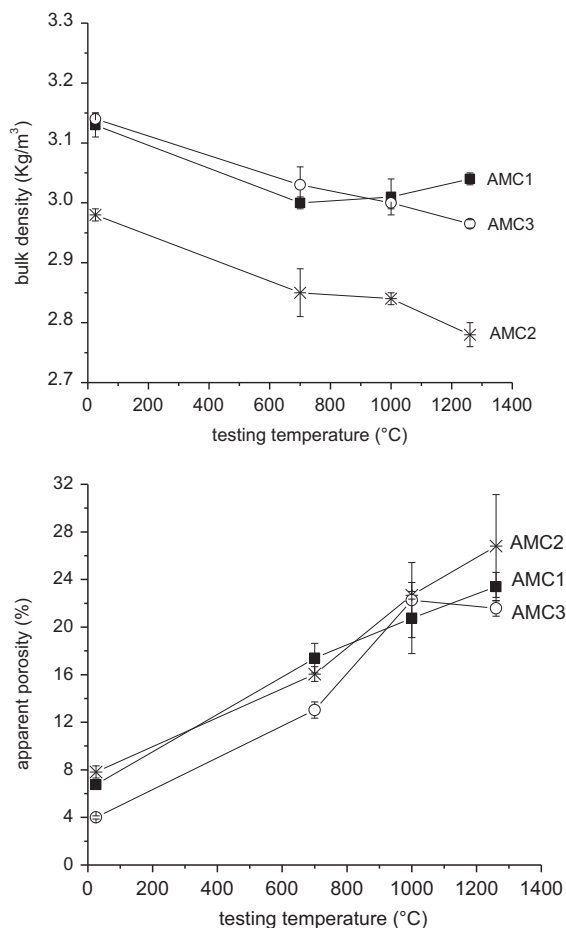


Fig. 5. Bulk density and apparent porosity of AMC refractories after mechanical tests at different temperatures.

In general, the global density diminished as testing temperature rose, with an opposite tendency to that of apparent porosity. This fact demonstrates that density is determined by the increase in open pores in most of cases, given that the processes occurring in the AMC materials (mainly the resin pyrolysis) lead to an increase in the solid density at least up to 1000 °C. The reactions at temperatures above 1000 °C lead to the increase or decrease of solid density depending on the reaction mechanism, which explains the higher global density of AMC1 after testing at 1260 °C in comparison with its value at 1000 °C.

3.2.2. Microstructural analysis

SEM images of the cross surfaces of cylinders tested at 1000 and 1260 °C are shown in Fig. 6. The phases identified by SEM/EDS in each case are reported in Table 2. The letter 'i' (indications) was used when the EDS compositions were not conclusive regarding the presence of the phase.

The surfaces of the specimens of the three materials tested at 1000 °C exhibited high deterioration of the matrix, which is associated mainly with the high porosity (open pores estimated in Fig. 5, plus the contribution of closed pores that were not quantified). However, chemical reactions previously established in

the thermal evolution analysis of the refractories [22,25], such as

$$4\text{Al}_{(l)} + \text{C}_{(s)} \rightarrow \text{Al}_4\text{C}_{3(s)} \quad (3)$$

and reaction (1), took place in mechanically tested specimens, since the solid phases, which were products of these reactions, were identified by SEM/EDS, as is reported in Table 2. Nevertheless, the local character of these phases seems to limit their contribution to matrix cohesion.

Although difficult to detect, 'holes', such as those shown in Fig. 7 for AMC1 tested at 1000 °C, were identified on the analyzed surfaces, which resemble the microstructure typically found as a consequence of the reactions (1) and (3) involving metallic aluminum [29]. Around the holes, the presence of Al_4C_3 formed by reaction (3) was detected for every refractory (Table 2). The fact that AlN was not identified in some cases is attributed to its localized formation as well as the difficulty in detecting light elements by EDS (the presence of nitride was confirmed by XRD). Aluminum nitride could be formed through the combination of the carbide with nitrogen from the flow [29]:



The appearance of AlN at a temperature lower than that at which aluminum carbide was detected (< 900 °C) was also reported [29], which could have formed due to the direct reaction between $\text{Al}_{(l)}$ and $\text{N}_{2(g)}$.

Regarding MgAl_2O_4 spinel (MA, formed by reaction (1)), EDS points with the composition of this phase were clearly identified in AMC1. Some holes in which MA composition was detected were seen in AMC2 whereas in AMC3, the percentage of spinel, when it was actually formed, was relatively small.

After mechanical tests at 1260 °C (Fig. 6), AMC1 was the refractory having the best surface quality. The degree of cohesion and continuity of the matrix was higher than those exhibited at 1000 °C, with the texture of the bonding phase clearly observed along with the presence of broken or damaged aggregates. Moreover, 'holes' distributed in the matrix were evident, as well as a foamy texture in the vicinity of some aggregates that could be associated with the presence of spinel [14,22]. Bearing in mind that the apparent porosity increased in AMC1 between 1000 and 1260 °C (Fig. 5), the higher cohesion was attributed to the advance of those reactions involving aluminum that lead to the formation of new phases such as spinel, as was determined in the analysis of the thermal evolution of AMC1 [22,25]. It was confirmed that spinel in these materials could be formed by different mechanisms [22,25], involving aggregates by reaction (2) for instance, as was also previously reported by other authors [14,15].

Meanwhile, the surfaces of AMC2 showed a great amount of the resin used to pack the samples in place of the matrix, even when compared with the specimens tested at 1000 °C, to the point that the typical microstructural features could not be identified. A foamy texture next to some aggregates could be observed in AMC2 as well. Something similar occurred with AMC3, but in this case, it was possible to detect damaged aggregates, some holes, and foamy regions in the vicinity of coarse alumina particles. In both AMC2 and AMC3, an increase in the apparent porosity occurred between 1000 and 1260 °C

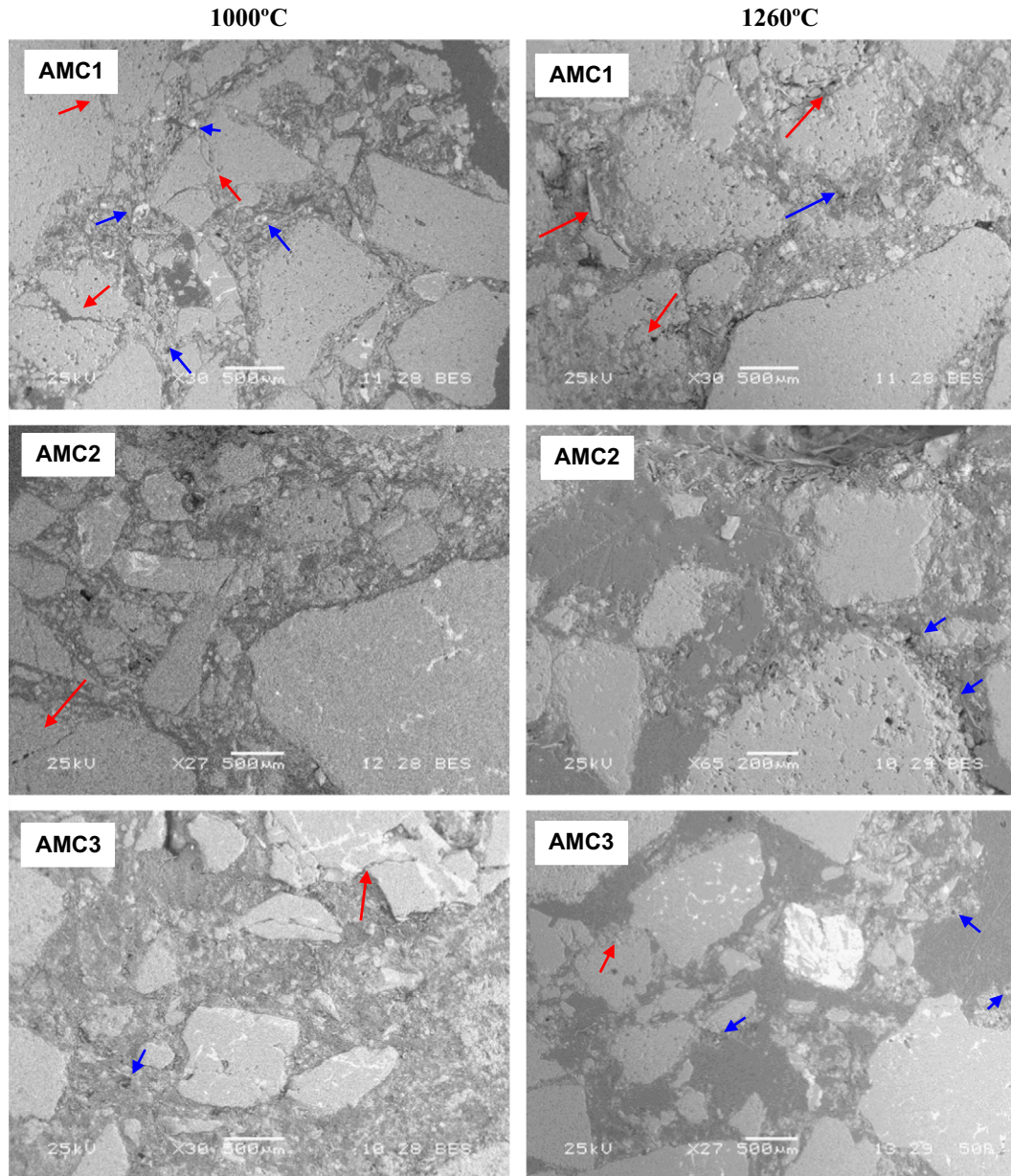


Fig. 6. Images of mechanically tested AMC specimens (SEM) at 1000 and 1260 °C; Black arrows (red arrow): cracks in aggregates; White arrows (blue arrows): possible 'holes'.

(Fig. 5), which explains the greater degradation of the respective matrices. Additionally, the reactions between the refractories' components took place, to a lower degree in AMC2 and AMC3 than in AMC1, similarly to what was already found in previous studies [22,25].

Conversely to what happened at 1000 °C, the microstructure of the 'holes' detected in the specimens tested at 1260 °C was very similar to those reported in the literature. This fact points out the increased advance of the processes leading to the formation of this characteristic texture at 1260 °C. Except for AMC2, in which only indications of the presence of aluminum carbide were found (Table 2), this phase was detected around the 'holes' in the other refractories. These results agree with the presence of Al_4C_3 reported by Baudín et al. inside MgO-C-Al

model and commercial refractories at 1200 °C under flowing argon [14,15], which disappeared at 1450 °C. Furthermore, the increase in the nitrogen content at EDS points in the outer regions of the tested cylinders could indicate the presence of AlN, likely formed by the decomposition of the carbide by reaction (4). At this temperature, the formation of $MgAl_2O_4$ around the 'holes' was evident in AMC1. However, there were only indications of the presence of spinel in AMC2 due to the degradation of the matrix (Fig. 6).

A high percentage of Si was observed in some EDS points of AMC3, as is shown in Fig. 8, and constituted the main components in some cases. This fact is consistent with the composition of the raw materials of this refractory, which contain bauxite, and the higher content of impurities, minor

SiO₂-containing phases in particular [22]. Since the presence of alkaline and earth alkaline elements such as Na, K and Ca (minor components of raw materials) were also detected, the presence of a glassy phase is likely. At increased magnification, the images of the AMC3 tested at 1260 °C generally show a microstructure with rounded edges and regions where small crystals seem immersed in a phase that could be a viscous one at the high temperature of the mechanical test (Fig. 8). These aspects were not clearly seen on the surfaces of AMC3 cylinders tested at 1000 °C.

4. Discussion

Before beginning the analysis of the particular characteristics of the mechanical behavior of each AMC refractory in the range of temperatures evaluated here, it is worth clarifying that the Young's modulus, such as it is determined in this work, is the result not only of the purely linear elastic strain (which should be more precisely measured during the unloading), but also of other types of strain, which can also contribute to its value. For this reason it has been named as 'apparent Young's modulus'. The *E* parameter defined in this paper is an indicator of the ability of the material to deform (in a reversible or irreversible way): the higher the modulus, the greater the stiffness and less deformable the material. The graphite (by sliding along the basal planes and the crumbling of flakes), pores (which contribute with a null Young's modulus) and microcracks of any origin (by their propagation) are considered

to be mainly responsible for the capacity of this type of refractory to deform. These same factors are which cause the deviation from linear behavior and the softening observed in the stress–strain curves at room temperature. The microcracking is considered the factor that determines the softening behavior: the coarse- to medium-sized particles act as obstacles in the extension of microcracks that run easier through the bonding phase due to its low cohesion.

On the other hand, mechanical strength is related to the type and/or the size of the flaws limiting the load bearing capacity of the refractory structure, in combination with the mechanical strength of the main components of the structure. In these refractories, flaws are commonly the discontinuities between the matrix–aggregates interfaces, and the microcracks and pores present in the bonding phase. However, despite the fact that fracture occurred preferably through the matrix, the cross surfaces of the specimens (Fig. 6) show some broken aggregates. Based on this fact, it is expected that that finest particles, which are less resistant, are involved in the material's failure.

At room temperature, the mechanical parameters of AMC refractories exhibited significant differences among them. AMC3 showed the highest value of the apparent Young's modulus, which is attributed mainly to its lower porosity (Table 1) and a higher affinity between resin and the rest of components of the matrix, as

Table 2
Phases identified in mechanically tested AMC refractories (1000 and 1260 °C).

	Temperature (°C)	Al ₄ C ₃	AlN	MgAl ₂ O ₄
AMC1	1000	x	–	xx
	1260	x	i ^a	xxx
AMC2	1000	x	i	xx
	1260	i	i	i
AMC3	1000	xx	–	xx
	1260	x	i	x

^a'i' (indications) is used when EDS analyses were not conclusive.

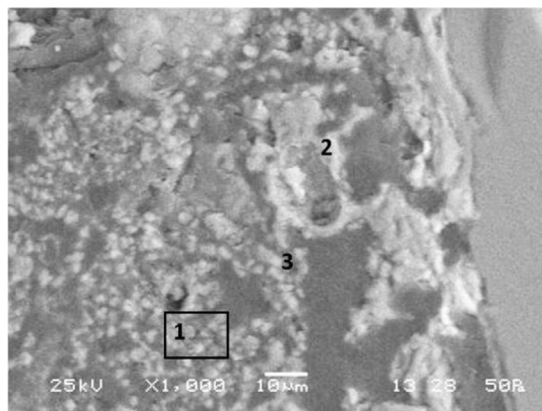


Fig. 8. Image of AMC3 specimen tested at 1260 °C showing a region with a high content of Si-containing phases: (1) Al or Al₂O₃+MA or Mg+phase with Si; (2) MA+3Al₂O₃.2SiO₂ (mullite); and (3) MA+phase with Al and Si.

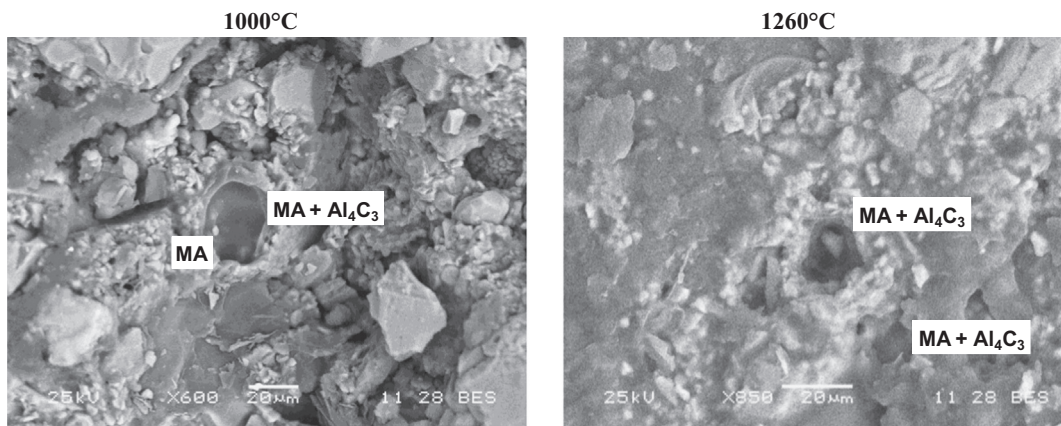


Fig. 7. SEM images where 'holes' in the microstructure are observed (AMC1, 1000 °C); MA:MgAl₂O₄.

was reported on the basis of the dilatometric behavior of this material [25]. Both factors would reduce the deformation undergone by AMC3 with respect to AMC1 and AMC2, as is deduced from its small fracture strain (Fig. 3). In AMC1, its lower graphite content and its higher proportion of tabular alumina (stiffer and more resistant than other sources of corundum such as brown electrofused alumina and bauxite) could contribute to the greater value of the Young's modulus of this refractory compared with that of AMC2. As for the mechanical strength, AMC1 and AMC3 exhibited similar values, partially due to the similarities in their mineralogical compositions. In the case of AMC2, the main reason for its lower mechanical strength is its higher porosity (pores and microcracks), which are the origin of a larger amount and/or size of flaws. Moreover, this material has the greatest proportion of magnesia and graphite, which are the least resistant inorganic phases. The degree of deviation from linearity of s – s curves, measured by the σ_Y/σ_R ratio (Fig. 4), was very similar in the three materials.

A significant decrease of the apparent Young's modulus and the mechanical strength is displayed in AMC1 and AMC3 plots as the testing temperature rose to 700 °C, which is expected taking into account the chemical and textural alterations taking place in the materials above 300 °C. According to results of a previous study on the oxidation of these refractories [28], graphite oxidation began before 700 °C in AMC1, but not in AMC3. This fact was confirmed in the post-testing inspection of specimens: a slight superficial decarburization was observed in AMC1, which was almost imperceptible in AMC3. Bearing this fact in mind, apart from the similar change in the apparent porosity (by formation and/or growth of pores and microcracks) of both refractories, this change – and not the loss of graphite – is considered to be the determining factor in the mechanical behavior of AMC1 and AMC3. On the other hand, any of the analyzed factors contribute to generating defects that reduce the structure's ability to bear a load: the increase in apparent porosity, the loss of graphite and the nucleation and extension of microcracks.

The fact that the value of the apparent Young's modulus in AMC2 was not modified in a significant way draws attention, considering that the open porosity (pores and microcracks) also increased in this refractory, retaining a large value at 700 °C as well (Fig. 5). On the other hand, the mechanical strength dropped (from the same causes mentioned above for the other two materials), together with a significant drop in the fracture strain. Possible justification for this behavior is found in the fact that AMC2 lost a proportion of graphite somewhat higher than AMC1 at 700 °C [28]. The loss of this component reduces the capacity of the structure to deform and could compensate for the increase in this ability due to its higher porosity.

An interesting aspect of the behavior of these materials is the decrease in the degree of deviation from linearity for AMC1 and AMC2, demonstrated by the increase of the σ_Y/σ_R ratio when the testing temperature changed from RT to 700 °C. These are the only refractories in which the oxidation of graphite was determined in this thermal condition, as this component was one of the main causes behind the non-linear s – s relationship. Even so, the degree of softening was significant in the three materials and was

attributed to the increased microcracking, which is a product of the matrix degradation caused by the resin pyrolysis.

When the testing temperature was increased to above 700 °C, none of the parameters seems to be dominated by porosity growth, even though it is considered to be the main cause of the severe degradation and low cohesion of the matrices of tested specimens (Fig. 6). An increase in mechanical strength was determined between 700 and 1000 °C in the three AMC refractories, which is attributed to the conversion of resin to a condensed C-structure (residual carbon) and the reactions leading to the crystallization of new solid phases (Table 2). Although of local character, the generation of chemical bonds between the different components of the refractory and the C-network increased the mechanical strength of the structure, mainly during the bonding phase, when the failure commonly begins. Nevertheless, the values of σ_R remained inferior to those at room temperature, in contrast to what was found in other AMC refractories of similar composition [19], which exhibited mechanical strength comparable or even higher at 1000 °C than at RT.

The differences in the extent of reactions taking place at $T > 1000$ °C among the three AMC materials did not seem have an effect on increasing their load bearing capacity between 700 and 1000 °C. The positive effect of these reactions could be offset by other processes occurring simultaneously. In the case of AMC1, which showed more advanced reactions, there was a deceleration in the advance of graphite oxidation [28], which is a low resistant component. Meanwhile, the graphite loss was manifest only between 700 and 1000 °C in AMC3.

On the other hand, the apparent Young's modulus showed a different change depending on the material: the value was unaltered in AMC1 and AMC3 and it decreased in AMC2. The behavior of the latter refractory could be dominated by the increase in the porosity, which is supposed to be higher than that shown in Fig. 5 (because it only quantifies open pores) and the subsequent degradation of the matrix (Fig. 6), more than the greater loss of graphite and the incipient formation of aluminum carbide and spinel (Table 2). In AMC1 and AMC3, these conflicting factors (growth of porosity, on one side, and graphite loss and new solid phase formation on the other) could offset each other, leading to the constancy of E parameter. In each case, the apparent Young's modulus at 1000 °C turned out to be lower than the value at RT, conversely to what is reported for AMC refractories of similar composition [19], whose values at 1000 °C were of the same order or notably higher than those at room temperature.

Taking into account experimental error, the fracture strain of AMC3 did not change in a significant way between 700 and 1000 °C although in AMC1 and AMC2, this parameter increased, more notably so in the latter. When the mechanical response is linear elastic, the fracture strain equals the ratio between mechanical strength and Young's modulus (Hooke's law). However, when the s – s behavior deviated strongly from linearity and/or there is softening of the structure, the fracture strain departs from the σ_R/E ratio. In AMC2, the remarkable increase of ε_R is considered a product of the simultaneous variation of the mechanical strength and the elastic modulus, but in opposite directions. In AMC1, the slighter increase in fracture strain could

be a consequence of the fact that only the fracture strength was increased. Conversely, the deviation of ε_R from the expected value in AMC3 is attributed to well-developed softening at 1000 °C, as well as the degree of non-linearity, which was somewhat higher than in the rest of materials (lower σ_Y/σ_R ratio). In this sense, an increased ability to accommodate volumetric variations in its structure was inferred from the dilatometric analysis of AMC3 [25], considered to be one of the responsible factors in the microcracking. If so, this process could promote the development of significant softening in AMC3.

Among 1000 °C and 1260 °C, the E parameter exhibited a significant increase for AMC1 and AMC2, higher in the former, and a decrease in AMC3. The mechanical strength changed similarly to the apparent Young's modulus in the first two refractories, whereas it increased slightly in AMC3. The fracture strain followed the change of the apparent Young's modulus in AMC1 and AMC2 in spite of the higher non-linearity of the s – s relationship (lower σ_Y/σ_R ratio) at 1260 °C in comparison with that at 1000 °C. This is attributed to the fact that softening was less or almost null in AMC1 and AMC2 at 1260 °C due to the reactions that took place in the matrix that made it more resistant to microcrack propagation.

The additional loss of graphite with respect to what occurred at 1000 °C in AMC1 and AMC2, besides the contribution of the new crystallized phases (which in this case included AlN), had a greater incidence of increase in E and σ_R than the growth of porosity and, likely, of microcracking. The increase was smaller in AMC2, which showed a more deteriorated bonding phase and possibly a lesser extent of reactions that lead to the formation of new phases (this could not be confirmed by SEM/EDS due to the loss of the matrix). Even so, the mechanical behavior was globally better at 1260 °C than at 1000 °C. It is possible that this was a consequence of the local formation of the new phases, which, even in this way, turned out to be very efficient in reducing the structure's flexibility despite the fact that the matrix as a whole deteriorated due to the loss of some of its components.

The behavior of apparent Young's modulus in AMC3 is related to the dominant effect of the increase in open porosity, the viscoplasticity and the microcracking, more than the crystallization of reaction products from Al-reactions. The presence of phases with high Si content at 1260 °C was observed in this refractory, which surely contributed to the deformation of the material by viscoplasticity and to the decrease in E as a consequence. Moreover, it could be that the activation of viscous flow requires an amount of stress greater than that needed to initiate microcracking, thus favoring the linearity of the s – s relationship (increase of σ_Y/σ_R ratio). On the other hand, the mechanical strength of AMC3 did not change significantly, indicating that the competition of the above-mentioned factors is different in relation to the critical defects distribution, which seems unaltered between 1000 and 1260 °C. The presence of an additional phase such as AlN or even crack closure [14] could be causes for the constancy of the mechanical strength of AMC3. As a product of the slight differences in σ_R and E , the fracture strain of AMC3 did not significantly change between 1000 and 1260 °C.

Bearing in mind the mechanical behavior of AMC refractories within the temperature range studied, AMC1 and AMC3 were the most resistant materials under thermal and mechanical loadings due to the lower proportion of graphite. Besides this feature, the higher amount of tabular alumina also contributes in AMC1, and the lower porosity and higher oxidation resistance of the graphite flakes contributes in the case of AMC3. Although AMC2 showed low stiffness and mechanical strength in general, these properties could be favorable in reducing the tendency of thermal shock damage to initiate and propagate. The flexibility of AMC materials (considering fracture strain as indicator) was different between the three refractories at RT and 700 °C, but it tended to become more similar at higher temperatures. Above 1000 °C, AMC3 showed constancy in this mechanical parameter, which could be related to its ability to absorb volumetric changes.

5. Conclusions

The mechanical evaluation of AMC refractories using stress–strain curves in compression gave a detailed description of their mechanical behavior up to 1260 °C in a non-oxidant atmosphere (nitrogen). Furthermore, through an exhaustive analysis of the mechanical parameter variations with temperature, together with data collected in the post-testing evaluation, the processes involved that determined the s – s relationship of each material were identified.

The thermal evolution of refractories' stiffness was determined by the increase in porosity coming from the formation of pores and cracks due to resin transformation, graphite loss, and microcracking up to 700 °C; at higher temperatures, the new solid phase formation (Al_4C_3 , AlN and $MgAl_2O_4$) and the viscoplasticity caused by the presence of Si-containing phases (only in AMC3 at 1260 °C) also contributed. The contribution of each factor strongly depended on the material's characteristics.

Changes in the mechanical strength with testing temperature, which were more homogeneous among AMC refractories than changes in the apparent Young's modulus, were controlled by processes that generate defects that are basically the same that determine the elastic parameter.

The degree of deviation from linear behavior was mainly determined by the graphite content and the contribution of microcracking, except in AMC3, in which the viscoplasticity also contributed (at the highest temperature). The evolution of the fracture strain as testing temperature increased was rather complex and strongly dependent on the refractory's quality, thus no general tendency could be found.

Acknowledgments

This work was supported by the Agencia Nacional de Promoción Científica y Tecnológica (ANPCyT) of Argentina under Project “Degradación termoquímica y termomecánica de refractarios óxido-C de uso siderúrgico” (PICT2006 No. 1887).

References

- [1] J. Poirier, Thermomechanical simulations of refractory linings – an overview, *Refract. Appl. News* 8 (2003) 16–22.
- [2] C.F. Cooper, The role of graphite in the thermal shock resistance of refractories, *J. Br. Ceram. Transit.* 84 (1985) 57–62.
- [3] Y. Kajita, S. Kariya, H. Kozuka, T. Honda, O. Shigetoshi, Development a method for quantitative assessment of flexibility and application for evaluating MgO–CaO–ZrO₂ bricks, in: *Proceedings of the UNITECR'97*, 1997, pp. 337–345.
- [4] M. Hampel, C.G. Aneziris, Evolution of microstructure and properties of magnesia-carbon refractories during carbonization: effect of grain size and graphite, *Ceram. Forum Int.* 84 (2007) E125–E131.
- [5] J.M. Robin, Y. Berthaud, N. Schmitt, J. Poirier, D. Themines, Thermo-mechanical behaviour of magnesia-carbon refractories, *Br. Ceram. Transit.* 97 (1998) 1–10.
- [6] S.A. Franklin, B.J.S. Tucker, Hot strength and thermal shock resistance of magnesia-carbon refractories, *Br. Ceram. Transit.* 94 (1995) 151–156.
- [7] E.M.M. Ewais, Carbon based refractories, *J. Ceram. Soc. Japan* 112 (2004) 517–532.
- [8] N. Schmitt, A. Burr, Y. Berthaud, J. Poirier, Micromechanics applied to the thermal shock behavior of refractory ceramics, *Mech. Mater.* 34 (2002) 725–747.
- [9] A.M. Fitchett, B. Wilshire, Mechanical properties of carbon-bearing magnesia-I. Pitch-bonded magnesia, *Br. Ceram. Transit. J.* 83 (1984) 54–58.
- [10] A.M. Fitchett, B. Wilshire, Mechanical properties of carbon-bearing magnesia-II. Pitch-bonded magnesia-graphite, *Br. Ceram. Transit. J.* 83 (1984) 59–62.
- [11] A.M. Fitchett, B. Wilshire, Mechanical properties of carbon-bearing magnesia-III. Resin-bonded magnesia and magnesia-graphite, *Br. Ceram. Transit. J.* 83 (1984) 73–76.
- [12] C. Baudín, C. Álvarez, Thermal history and mechanical behaviour of MgO–C based refractories, in: *Proceedings of the UNITECR'95*, 1995, pp. 84–91.
- [13] S. Uchida, K. Ichikawa, High-temperature properties of unbaked MgO–C bricks containing Al and Si Powders, *J. Am. Ceram. Soc.* 81 (1998) 2910–2916.
- [14] C. Baudín, C. Álvarez, R.E. Moore, Influence of chemical reactions in magnesia – graphite refractories: I. Effects on texture and high temperature mechanical properties, *J. Am. Ceram. Soc.* 82 (1999) 3529–3538.
- [15] C. Baudín, C. Álvarez, R.E. Moore, Influence of chemical reactions in magnesia – graphite refractories: II. Effects of aluminum and graphite contents in generic products, *J. Am. Ceram. Soc.* 82 (1999) 3539–3548.
- [16] C. Baudín, High temperature mechanical behavior of magnesia-graphite refractories, in: J. Bennett, J.D. Smith (Eds.), *Fundamentals of Refractory Technology*, Ceramic Transactions, vol. 125, The American Ceramic Society, Westerville, 2001, pp. 73–92.
- [17] L. Musante, L.F. Martorello, P.G. Galliano, A.L. Cavalieri, A.G. Tomba Martinez, Mechanical behavior of MgO–C refractory bricks evaluated by stress–strain curves, *Ceram. Int.* 38 (2012) 4035–4047.
- [18] C. Taffin, J. Poirier, The behaviour of metal additives in MgO–C and Al₂O₃–C refractories, *Interceram* 43 (1994) (354–358, 458–460).
- [19] L. Musante, V. Muñoz, M.H. Labadie, A.G. Tomba Martinez, High temperature mechanical behavior of Al₂O₃–MgO–C refractories for steelmaking use, *Ceram. Int.* 37 (2011) 1473–1483.
- [20] D.A. Bell, F.T. Palín, Measurement of high temperature mechanical properties of refractories containing carbon, in: *Proceedings of UNITECR'89*, 1989, pp. 1219–1124.
- [21] V. Muñoz, G.A. Rohr, A.L. Cavalieri, A.G. Tomba Martinez, Experimental methodology of the mechanical evaluation of oxide-carbon refractories by strain measurement, *J. Test. Eval.* 40 (1) (2012) <http://dx.doi.org/10.1520/JTE103420>.
- [22] V. Muñoz, P. Pena, A.G. Tomba Martinez, Physical, chemical and thermal characterization of alumina–magnesia–carbon refractories, *Ceram. Int.* 40 (2014) 9133–9149.
- [23] V. Muñoz, G.A. Rohr, A.G. Tomba Martinez, A.L. Cavalieri, Aspectos experimentales de la determinación de curvas esfuerzo-deformación a alta temperatura y en atmósfera controlada: refractarios Al₂O₃–MgO–C, *Bol. Soc. Esp. Cerám. Vidr.* 50 (3) (2011) 125–134.
- [24] DIN EN 993-1 (DIN 51056), Method of test for dense shaped refractory products, Determination of bulk density, apparent porosity and true porosity, 1995.
- [25] V. Muñoz, A.G. Tomba Martinez, Thermal evolution of Al₂O₃–MgO–C refractories, *Procedia Mater. Sci.* 1 (2012) 410–417.
- [26] S.K. Sadmezhaad, S. Mahshid, B. Hasemi, Z.A. Nematí, Oxidation mechanism of C in MgO–C refractory bricks, *J. Am. Ceram. Soc.* 89 (2006) 1308–1316.
- [27] B. Rand, B. McEnaney, Carbon binder from polymeric resins and pitch. Part I – pyrolysis behaviour and structure of the carbons, *J. Br. Ceram. Trans.* 84 (1985) 157–165.
- [28] V. Muñoz, L. Musante, P.G. Galliano, E. Brandaleze, A.G. Tomba Martinez, Chemical wear of Al₂O₃–MgO–C bricks by air and basic slags, in: *Proceedings of the UNITECR 2013*, 2013.
- [29] S. Zhang, N.J. Marriot, W.E. Lee, Thermochemistry and microstructures of MgO–C refractories containing various antioxidants, *J. Eur. Ceram. Soc.* 21 (2001) 1037–1047.
- [30] P.O.R.C Brant, B. Rand, Reactions of silicon and aluminum in MgO–graphite composites: I – effects on porosity and microstructure, in: *Proceedings of the UNITECR'91*, 1991, pp. 172–174.